Journal of
MATERIALS RESEARCH

Bismuth quantum-wire arrays fabricated by a vacuum melting and pressure injection process

Zhibo Zhang
Department of Physics, Massachusetts Institute of Technology, Cambridge, Massachusetts 02139-4307

Jackie Y. Ying[a)]
Department of Chemical Engineering, Massachusetts Institute of Technology, Cambridge, Massachusetts 02139-4307

Mildred S. Dresselhaus
Department of Electrical Engineering and Computer Science and Department of Physics, Massachusetts Institute of Technology, Cambridge, Massachusetts 02139-4307

(Received 12 September 1997; accepted 13 October 1997)

Ultrafine bismuth nanowire arrays were synthesized by injecting its liquid melt into nanochannels of a porous anodic alumina template. A large area (1 cm × 1.5 cm) of parallel wires with diameters as small as 13 nm, lengths of 30–50 μm, and packing density as high as 7.1×10^{10} cm^{-2} has been fabricated. X-ray diffraction patterns revealed these nanowires, embedded in the insulating matrix, to be essentially single crystalline and highly oriented. The optical absorption spectra of the nanowire arrays indicate that these bismuth nanowires undergo a semimetal-to-semiconductor transition due to two-dimensional quantum confinement effects.

Highly regular metal and semiconductor nanowire arrays embedded in a dielectric matrix have attracted a great deal of research attention because of their potential applications in electronic and optical devices and promise for studying one-dimensional (1D) quantum properties. The quantum confinement of carriers in two dimensions will significantly change their electronic energy states and make the properties of these 1D systems very different from their bulk counterparts. A promising approach to fabricate nanowire systems is to fill an array of nanochannels with the media of interest. Porous anodic alumina,[1–3] which has hexagonally packed nanometer-sized channels, is one such possible host template. Besides its desirable geometry, the wide band gap energy of alumina makes it an excellent host material for quantum wires. Anodic alumina has previously been used to synthesize a variety of metal and semiconductor nanowires, such as Ni, Pd, Au, Pt, and CdS, through chemical or electrochemical processes.[4–7] However, the diameters of those nanowires have not reached the quantum confinement regime. In order to exhibit strong quantum confinement characteristics, the wire diameter should be smaller than the exciton diameter, which is given by $d_{ex} = 2\epsilon\hbar^2 (m_e^{-1} + m_h^{-1})/e^2$, where ϵ is the static dielectric constant, and m_e and m_h are the effective masses of electrons and holes, respectively. Bismuth, which is a semimetal and has a very small electron effective mass ($m_e \approx 0.014m_0$ at the band edge along the trigonal direction, and $m_e \approx 0.0036m_0$ for heavy electrons along the bisectrix direction), is considered a good candidate to study quantum confinement effects in the 1D system. Our theoretical calculations estimate that Bi makes a transition from a semimetal to a 1D semiconductor at a wire diameter of about 45 nm or 81 nm if the wire is oriented along the trigonal direction or the bisectrix direction, respectively.[8]

In this paper, Bi quantum-wire arrays were fabricated by a novel vacuum melting and pressure injection technique which can produce continuous, dense nanowire arrays, as required by many practical electronic applications. High-pressure injection of molten metal has been used to fill a single glass nanotube,[9] and more recently, porous anodic alumina having channel diameters larger than 200 nm.[10] The injection rate at time t is given by[11]:

$$l(t) = \sqrt{(P_a + 2\gamma_{lv}\cos\theta/r)(r^2 + 4\nu \times r)t/(4\eta)}, \quad (1)$$

where P_a is the external pressure, γ_{lv} is the liquid-vapor surface tension, θ is the contact angle, r is the channel radius, η is the viscosity of the liquid, and ν is its coefficient of slip. θ is determined by Young's equation[12]: $\gamma_{lv}\cos\theta = \gamma_{sv} - \gamma_{sl}$, where γ_{sv} and γ_{sl} are the solid-vapor and solid-liquid surface tensions, respectively. For a ceramic/metal melt system, the difference between γ_{sv} and the solid-vacuum surface tension γ_{so} is negligible. Through simple thermodynamic calculations, we end up with the relation: $\cos\theta = (2V_{sl}/V_{ll}) - 1$,

[a)]Author to whom correspondence should be addressed.

where V_{sl} and V_{ll} are the solid-liquid and liquid-liquid interaction energies, respectively. In previous studies,[9,10] θ was assumed to be close to 180° since V_{ll} is very high for a metallic liquid. However, V_{sl} is not always small compared to V_{ll}, and by selectively changing the surface composition of the channel wall, it should be possible to reduce θ for a given liquid. For an anodic alumina template, it is known that the surface of the alumina channels is contaminated by anions from the anodizing electrolyte[13]; thus V_{sl} may be enhanced for a specific metal melt by using a suitable electrolyte. This is exactly what we achieved in our study. By preparing an anodic alumina template using a sulfuric acid solution as the electrolyte, molten Bi was successfully driven into channels with diameters as small as 13 nm at a pressure of only 315 bar. Since the surface tension of Bi is about 375 dyn/cm, a pressure of 1150 bar would have been needed to fill 13-nm channels if we assume that $\theta = 180°$. Operating at such a high pressure at the melting temperature of Bi (T_m = 271.5 °C) would have greatly complicated the filling of the channels with ultrafine diameters using a conventional experimental setup.

An outline of the fabrication process is presented in Fig. 1. The porous template was generated by anodizing a mechanically and electrochemically polished high-purity aluminum substrate (99.99+%) in a 4 wt.% oxalic acid solution or a 20 wt.% sulfuric acid solution as the electrolyte. Each nanochannel in Fig. 1(a) has only one opening entrance due to the presence of the dense alumina barrier layer between the nanochannels and the Al substrate. After a brief thermal treatment, the porous film, which was kept on the Al substrate, was placed inside a high pressure reactor chamber and surrounded by high-purity (99.999%) Bi pieces. To degas the porous film, the reactor chamber was evacuated to $\sim 10^{-2}$ mbar while heated to a temperature slightly lower than T_m, the melting point of Bi. After the film was degassed, the temperature of the reactor was raised above T_m. The vacuum pump was then disconnected, and high-pressure argon gas was introduced to drive the molten Bi into the evacuated channels of the anodic alumina host. The low T_m of Bi and the high thermal stability (up to 800 °C[14]) and rigidity of the anodic alumina film make this filling process possible. After the injection process was completed, the reactor was slowly cooled down to room temperature, and the impregnated Bi was solidified and crystallized inside the nanochannels. The pressure was then slowly released. Next, the sample [Fig. 1(b)] was mechanically extracted from the surrounding Bi metal, and the Al substrate was etched away by an amalgamation process.[15] The barrier layer was dissolved using a 4 wt.% phosphoric acid solution to yield the final Bi-filled anodic alumina film sample shown in Fig. 1(c).

In this work, we prepared films with channel diameters of 56 ± 9.3 nm (anodized in oxalic acid), 23 ± 6.7, and 13 ± 4.3 nm (anodized in sulfuric acid) and channel densities of 7.4×10^9 cm^{-2}, 4.6×10^{10} cm^{-2}, and 7.1×10^{10} cm^{-2}, respectively. These dimensions were determined from transmission electron microscopy (TEM) images of the films, after they were thinned from both sides by argon ion milling. As an example, Fig. 2 shows one of these TEM images.

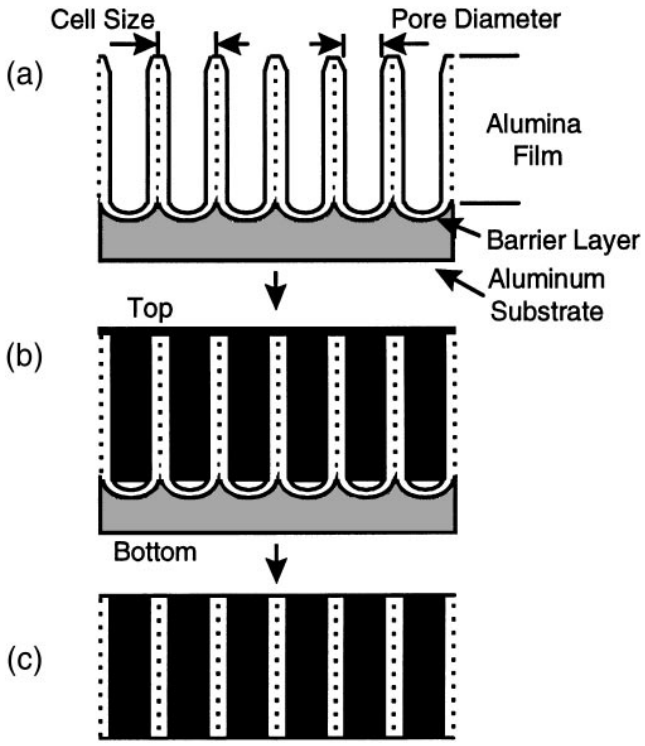

FIG. 1. Schematic diagram of the fabrication process of the nanowire array composite: (a) an as-prepared porous anodic alumina template, (b) pressure injection of molten metal into evacuated channels of the porous template, and (c) the metal-filled composite film which can be used in practical applications.

To confirm that the nanochannel arrays have been filled by continuous dense Bi nanowires, the alumina matrix was dissolved in a solution of phosphoric acid and chromic acid, which did not attack the Bi nanowires. Figure 3(a) shows a typical SEM image of the Bi-filled films after the alumina matrix was partially dissolved from the bottom side of the film to expose the Bi wires. The portion of the nanowires without support tended to agglomerate with and adhere to each other, making it difficult to resolve the individual wires. Although bulk Bi is very brittle, the Bi nanowires were amazingly ductile, indicating their excellent crystallinity. Since the whisker-like features shown in Fig. 3(a) were observed throughout the entire film, we conclude that most of the channels have been filled by Bi. In order to further resolve individual wires, we fully dissolved the alumina matrix to make freestanding Bi wires. Figures 3(b)

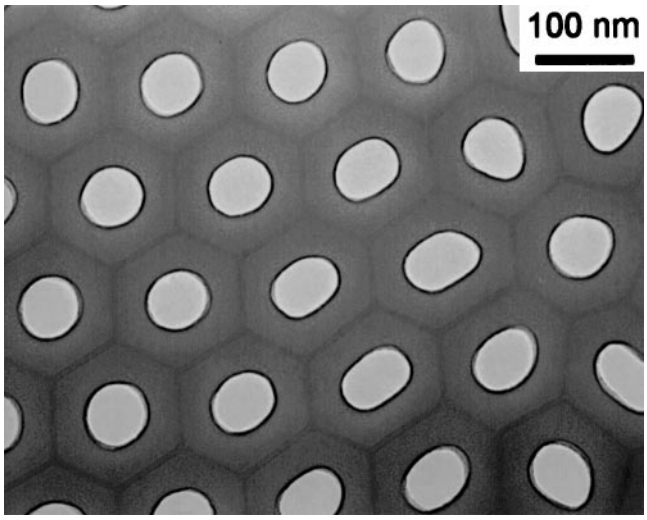

FIG. 2. TEM image of the cross section of the anodic alumina template with an average channel diameter of 56 nm after ion milling (argon ions at 6 keV).

and 3(c) show TEM images of such freestanding Bi nanowires.

Shown in Fig. 4 are x-ray diffraction (XRD) patterns of the Bi-filled films (taken from the bottom side) after removal of the barrier layer. All the XRD peaks are located very close to the peak positions of 3D bulk Bi, revealing that the rhombohedral lattice structure of bulk Bi is also preserved in the nanowires. The XRD peaks are very narrow and no peak broadening was observed within the instrumental limit, which indicates long-range periodicity of the lattice structure along the wire. For the sample which was synthesized from a template with an average pore diameter of 56 nm, only three strong peaks [(012), (110), and (202)] were observed [Fig. 4(a)]. For the samples with diameters of 23 and 13 nm, only (012) and (024) peaks were found [Figs. 4(b) and 4(c)]. We therefore conclude that these individual Bi nanowires are essentially single crystal and are similarly oriented. This single-crystal orientation of the array of Bi nanowires will be very important for many applications involving the transport properties of 1D Bi nanowires. The single crystallinity is also confirmed by selected-area electron diffraction experiments, and a detailed study of the crystal structure of the Bi nanowires will be reported in a subsequent paper.

The porous alumina film, which is clear and transparent originally, changed color after it was filled with Bi, with a color that depends on the diameter of the Bi nanowires. The samples with Bi nanowire diameters of 56 nm, 23 nm, and 13 nm are dark, yellowish, and near transparent, respectively. Figure 5 shows the optical absorption spectra of these Bi nanowire composite films and their corresponding unfilled anodic alumina templates. The composite film

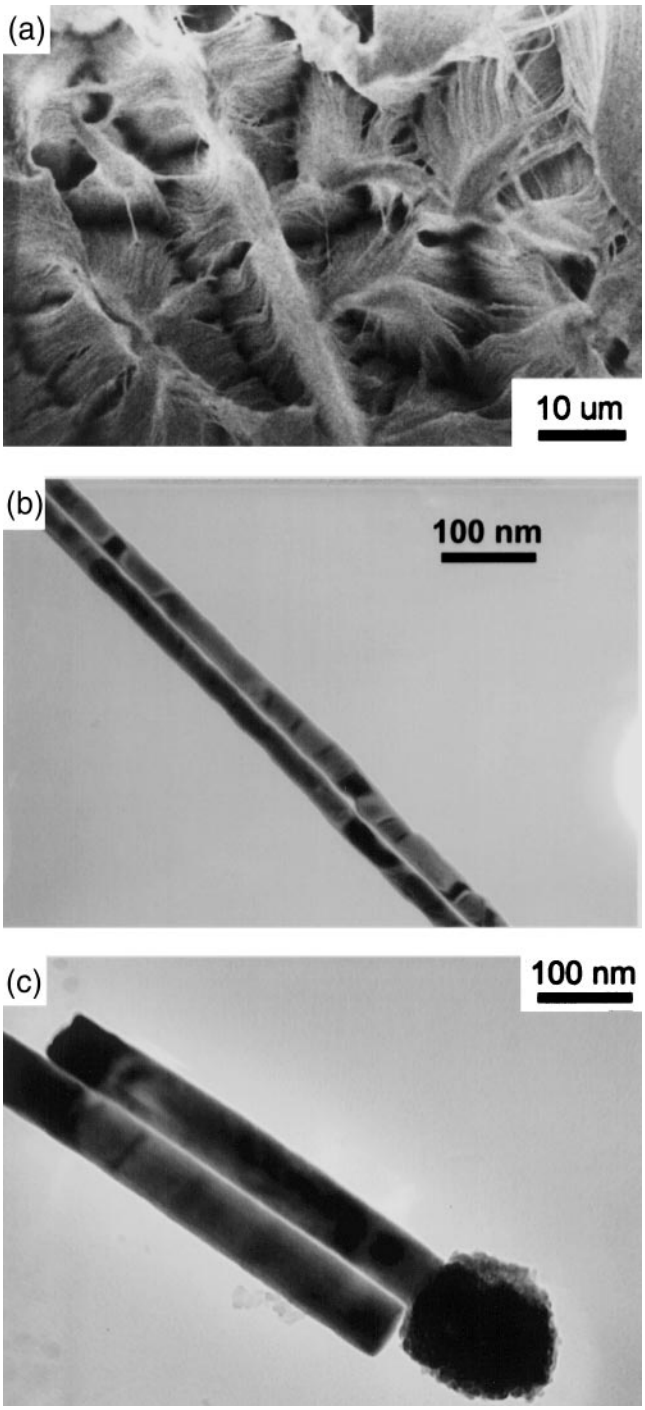

FIG. 3. (a) SEM micrograph of the exposed Bi nanowires after the alumina matrix was partially dissolved from the bottom side of the film. (b, c) TEM images of the freestanding Bi nanowires. Shown are Bi nanowires prepared from templates with average channel diameters of (a, b) 23 nm and (c) 56 nm.

with 56-nm diameter nanowires is opaque over the entire wavelength range [Fig. 5(a)], representing a metal or a narrow band gap semiconductor, while the composite films with nanowires of 23-nm and 13-nm

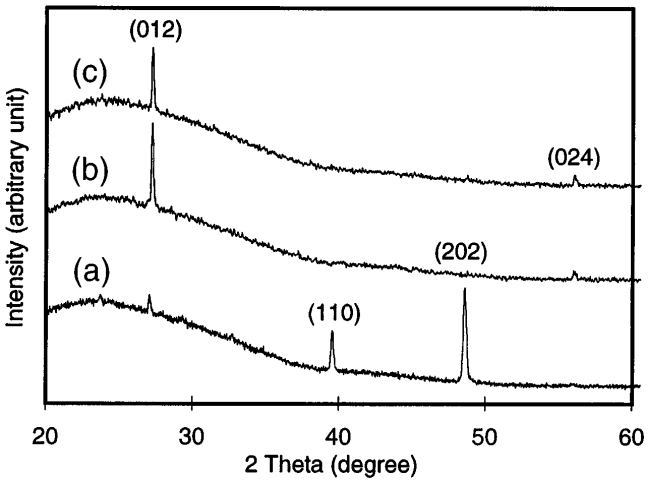

FIG. 4. XRD patterns of the Bi nanowire/anodic alumina composites made from templates with average channel diameters of (a) 56 nm, (b) 23 nm, and (c) 13 nm. Marked above individual peaks are the Miller indices of the corresponding lattice planes.

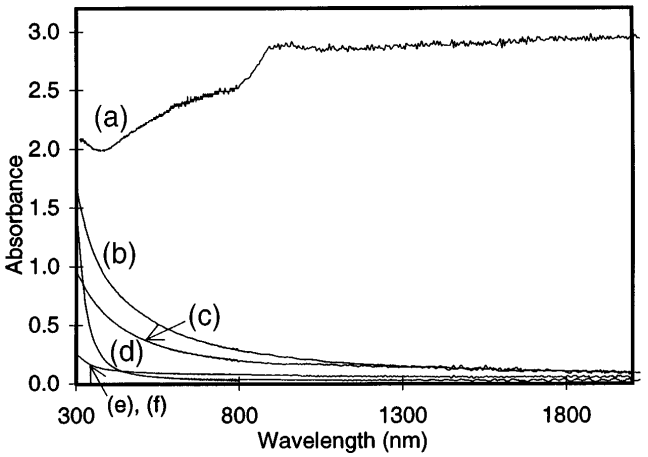

FIG. 5. The room-temperature optical absorption spectra of the Bi nanowire/anodic alumina composite films with average wire diameters of (a) 56 nm, (b) 23 nm, and (c) 13 nm, and the corresponding unfilled anodic alumina templates (d), (e), and (f).

diameters have an absorption edge at the short wavelength [Figs. 5(b) and 5(c)], the signature of a semiconductor, and the absorption edge is blue-shifted from (b) to (c) with decreasing wire diameter. These differences in the optical absorption spectra cannot be explained by the effective medium theory,[16] which does account for the color changes observed in other metal-ceramic composite films.[17] The results of Fig. 5 indicate a dramatic change in the band gap energy of the Bi nanowires as a function of wire diameter. They are consistent with our theoretical expectations[8] that a Bi nanowire makes a semimetal-to-semiconductor transition as the electron gas experiences quantum confinement in the two directions normal to the wire.

Considering the high thermal and chemical stability of the anodic alumina template, the process of the pressure injection of molten Bi into the evacuated channels described in this paper can be applied to other low melting temperature metals, semiconductors, alloys, polymers and gels. The resulting nanowire array composites, especially the 1D Bi quantum wire systems, are expected to lead to interesting applications in thermoelectricity, magnetoresistance, and other electronic and optical devices.

ACKNOWLEDGMENTS

We thank the National Science Foundation (CTS-9257223, DMR-9400334) and the U.S. Navy (N00167-92-K0052) for financial support, and L. Zhang and X. Sun of MIT for valuable discussions.

REFERENCES

1. F. Keller, M. S. Hunter, and D. L. Robinson, J. Electrochem. Soc. **100**, 411 (1953).
2. K. Itaya, S. Sugarwara, K. Arai, and S. Saito, J. Chem. Engr. Jpn. **17**, 514 (1984).
3. R. C. Furneaux, W. R. Rigby, and A. P. Davidson, Nature (London) **337**, 147 (1989).
4. M. Saito, M. Kirihara, T. Taniguchi, and M. Miyagi, Appl. Phys. Lett. **55**, 607 (1989).
5. M. Konno, M. Shindo, S. Sugawara, and S. Saito, J. Mem. Sci. **37**, 193 (1988).
6. C. R. Martin, Science **266**, 1961 (1994).
7. D. Routkevitch, T. Bigioni, M. Moskovits, and J. M. Xu, J. Phys. Chem. **100**, 14037 (1996).
8. Z. Zhang, X. Sun, M. S. Dresselhaus, J. Y. Ying, and J. P. Heremans, unpublished.
9. M. Gurvitch, J. Low Temp. Phys. **38**, 777 (1980).
10. C. A. Huber, T. E. Huber, M. Sadoqi, J. A. Lubin, S. Manalis, and C. B. Prater, Science **263**, 800 (1994).
11. E. W. Washburn, Phys. Rev. **17**, 372 (1921).
12. P. G. de Gennes, Rev. Mod. Phys. **57**, 827 (1985).
13. G. E. Thompson, R. C. Furneaux, G. C. Wood, J. A. Richardson, and J. S. Goode, Nature (London) **272**, 433 (1978).
14. P. P. Mardilovich, A. N. Govyadinov, N. I. Mukhurov, A. M. Rzhevskii, and R. Paterson, J. Mem. Sci. **98**, 131 (1995).
15. J. P. O'Sullivan and G. C. Wood, Proc. Roy. Soc. London A **317**, 511 (1970).
16. D. E. Aspnes, Thin Solid Films **89**, 249 (1982).
17. C. A. Foss, Jr., G. L. Hornyak, J. A. Stockert, and C. R. Martin, J. Phys. Chem. **96**, 7497 (1992).